Ultimate limit of resolution of subwavelength imaging devices formed by metallic rods

Mário G. Silveirinha,[1,*] Pavel A. Belov,[2] and Constantin R. Simovski[3]

[1]*Department of Electrical Engineering, Instituto de Telecomunicações, University of Coimbra, 3030 Coimbra, Portugal*

[2]*Department of Electronic Engineering, Queen Mary University of London, Mile End Road, E1 4NS, London, UK*

[3]*Radio Laboratory, Helsinki University of Technology, P.O. Box 3000, FI-02015 TKK, Finland*

**Corresponding author: mario.silveirinha@co.it.pt*

Received April 14, 2008; accepted April 25, 2008;
posted June 18, 2008 (Doc. ID 95042); published July 29, 2008

It is demonstrated that the ultimate physical limit of resolution of novel imaging devices based on arrays of metallic rods is determined by the skin depth of the metal. Our theoretical and numerical results show that wire medium lenses may provide a unique solution for subwavelength imaging at frequencies up to the terahertz range and may enable image formation at a significant distance from the source plane. © 2008 Optical Society of America

OCIS codes: 110.0110, 050.6624, 160.1245.

Conventional lenses operate only with the far field of the source, formed by propagating spatial harmonics. The information related to the near field is associated with evanescent spatial harmonics, which exhibit exponential decay in all natural materials as well as in free space. Thus, the near field is not directly accessible with conventional imaging systems, and details smaller than a half-wavelength of radiation cannot be resolved.

The near field can be scanned, point by point, using small near-field probes. However, scanning near-field microscopy is a rather slow process, and thus lenses that may enable the simultaneous imaging of the whole region of interest with superresolution are of great practical interest. Several solutions, such as silver superlenses [1], hyperlenses [2,3], and stimulated emission depletion (STED) fluorescence microscopes [4], have recently been proposed for this effect.

Other theoretical and experimental studies have demonstrated that arrays of parallel metallic rods may enable subwavelength imaging in a wide frequency range that encompasses microwaves, terahertz, and IR frequencies [5,6]. Such imaging devices may be regarded as a bundle of very subwavelength waveguides performing pixel to pixel imaging. Thus it is usually assumed that the resolution of such systems is determined mainly by the lattice constant, a, that defines the distance between the wires. It was theoretically demonstrated in [7] that for perfectly electric conducting (PEC) wires the resolution is approximately $2a$. Hence, for PEC wires the resolution may be made as small as desired as compared to the wavelength in free space. Even though the PEC approximation may be very accurate at microwaves, at higher frequencies the effect of losses and the plasmonic response of metals cannot be neglected. In this Letter it is theoretically demonstrated that for real metals (with finite conductivity) the resolution of the "wire medium lens" cannot be further improved by reducing the spacing between the wires after the radius of the wires becomes smaller than the skin depth of the metal.

The anomalous imaging potentials of wire media may be explained in light of the extreme optical anisotropy provided by long parallel metallic wires. Indeed, in the very long wavelength limit such structured material may be characterized by the dielectric function

$$\bar{\bar{\varepsilon}} = \varepsilon(\hat{\mathbf{u}}_x\hat{\mathbf{u}}_x + \hat{\mathbf{u}}_y\hat{\mathbf{u}}_y) + \infty\hat{\mathbf{u}}_z\hat{\mathbf{u}}_z, \qquad (1)$$

where ε is the permittivity of the host matrix. Materials with extreme anisotropy have remarkable properties: All the extraordinary waves supported by the medium are propagating waves and have the same phase velocity along the optical axis. This property may enable the propagation of an arbitrary field distribution with suitable polarization through such material with no loss of resolution, when the thickness of the slab is tuned to obey the Fabry–Perot (FP) condition [5,6]. In the wire medium the extraordinary waves described by Eq. (1) are the so-called transmission line or transverse electromagnetic (TEM) modes [8]. Strictly speaking, the permittivity model [Eq. (1)] is only a first-order approximation, because the wire medium is spatially dispersive [8].

Remarkably, in a material with extreme anisotropy the FP condition is verified simultaneously for all spatial harmonics, because the extraordinary waves travel along the slab with the same phase velocity, independent of the transverse wave vector. Thus, the total electrical length of the slab remains the same for all possible incidence angles. This collective resonance ensures perfect imaging and is known as the canalization regime [9].

In what follows we study how the finite conductivity of the rods limits the resolution of the imaging system. It is supposed that the metallic rods are aligned along the z direction and have radius R and relative permittivity ε_m. Following [10], the response of metals up to optical frequencies may be modeled using a Drude dispersion characteristic $\varepsilon_m = 1-[\omega_m^2/\omega(\omega-j\Gamma)]$, where ω_m is the plasma frequency and Γ is the collision frequency. For simplicity, in the following analysis the host medium is assumed to be air.

The quasi-TEM electromagnetic mode that enables canalization has propagation constant along z such that $k_z = k_z(\omega, k_\parallel)$, where $\mathbf{k}_\parallel$ is the transverse wave vector (the Fourier variable in the image plane). The canalization effect requires that $k_z = k_z(\omega, k_\parallel)$ be nearly independent of $k_\parallel$ [9]. From the theoretical analysis of [6] it is known that

$$k_z^{(0)} = k_z|_{k_\parallel=0} \approx \frac{\omega}{c}, \quad k_z^{(\infty)} = k_z|_{k_\parallel=\infty} = \sqrt{\left(\frac{\omega}{c}\right)^2 + \beta_c^2}, \qquad (2)$$

where c is the speed of light in vacuum and the parameter β_c is given by $\beta_c^2 = -[\beta_p^2/(\varepsilon_m - 1)f_V]$. In the previous formula, $f_V = \pi R^2/a^2$ is the volume fraction of the metal and β_p is the plasma wavenumber defined as in [6]. For the case of a perfect conductor, $\varepsilon_m = -\infty$, the parameter β_c is exactly zero, and thus $k_z(\omega, k_\parallel)$ becomes independent of $k_\parallel$.

This is the ideal case for operation in the canalization regime. However, for realistic metals, especially at terahertz frequencies and above, β_c is different from zero and the quasi-TEM mode is not exactly dispersionless [6]. The parameter $k_z^{(\infty)}/k_z^{(0)}$ can be used to characterize this effect. If $k_z^{(\infty)}/k_z^{(0)}$ is close to unity the effect of the finite conductivity may be considered negligible, otherwise it may severely affect the imaging quality. It is simple to verify that

$$\frac{k_z^{(\infty)}}{k_z^{(0)}} \approx \sqrt{1 + \frac{c^2(1 - j\Gamma/\omega)}{\omega_m^2 R^2}\frac{(\beta_p a)^2}{\pi}}. \qquad (3)$$

The parameter $\beta_p a$ depends only on the ratio R/a, and for typical designs $1.0 < \beta_p a < 2.5$. Thus, Eq. (3) demonstrates that $k_z^{(\infty)}/k_z^{(0)}$ is close to unity only if

$$\frac{c}{\omega_m R}(1 + (\Gamma/\omega)^2)^{1/4} \ll 1. \qquad (4)$$

On the other hand, the skin depth of the metal is given by

$$\delta = \frac{-c}{\omega \operatorname{Im}\{\sqrt{\varepsilon_m}\}} \approx \frac{c}{\omega_m}(1 + (\Gamma/\omega)^2)^{1/4}\frac{1}{\cos\left(\frac{1}{2}\arctan\left(\frac{\Gamma}{\omega}\right)\right)}.$$

Thus, Eq. (4) is equivalent to $\delta \ll R$. Therefore, we conclude that plasmonic and loss effects are negligible, provided the skin depth of the metal is smaller than the radius of the rods. When $R < \delta$ the resolution cannot be further improved by reducing the lattice constant. Since for lenses with PEC rods the resolution is approximately $2a$ [7], and given that $a > 2R$, one may estimate that the ultimate physical limit of resolution of wire medium lenses is about 4 times the skin depth of the material. The limits of resolution yielded by rods of silver (Ag), gold (Au), aluminum (Al), and copper (Cu) at several frequencies are compiled in Table 1.

At microwave frequencies the ultimate limit of resolution is several orders of magnitude larger than the classical diffraction limit, and the best results are achieved with silver. Even at terahertz frequencies the resolution may be of the order of $\lambda/300$.

To support these theoretical findings the performance of a wire medium lens at 5 THz was numerically simulated. The wires were assumed to be made of silver. The effect of realistic losses in silver was fully taken into account in all the simulations [10]. In the first example, the lattice constant is $a = 0.04\lambda_0$, the thickness of the lens is $L = 0.5\lambda_0$, and the rods stand in air. The image is created by a plane wave (with magnetic field along y) that illuminates an opaque metallic screen with a very subwavelength slit along the y direction. The wire medium lens is located at a distance $d_1 = 0.01\lambda_0$ from the opaque plane. The image plane is located at a distance $d_2 = d_1$ from the back interface of the lens. For simplicity, it is assumed that the structure is periodic along the y direction. Within these conditions, the magnetic field H_y squeezed through the tiny slit is very similar to the field created by a magnetic line current located at the position of the slit. Thus, a simple analysis demonstrates that H_y at the image plane is such that

$$H_y(x) \sim \frac{1}{\pi}\int_0^\infty \frac{e^{-\gamma_0(d_1+d_2)}}{2\gamma_0} T(k_x)\cos(k_x x)\mathrm{d}k_x, \qquad (5)$$

where $\gamma_0 = \sqrt{k_x^2 - (\omega/c)^2}$ and $T(k_x)$ is the transfer function of the wire medium slab, which can be evaluated using formula (20) of [6]. In Fig. 1 the normalized H_y is plotted at the image plane for different values of R. The solid thin curves represent the profiles calculated using the analytical formula [Eq. (5)], whereas the dashed curves were obtained using the full-wave electromagnetic simulator CST Microwave Studio considering that the number of wires along the x direction is 28. The agreement between the two sets of results is quite reasonable. The results of Fig. 1 show that for a fixed lattice constant a the resolution of the

Table 1. Ultimate Limit of Resolution of Wire Medium Slabs for Several Metals and Frequencies[a]

	100 MHz	1 GHz	10 GHz	100 GHz	1 THz	10 THz
Ag	$\lambda/116000$ (26 μm)	$\lambda/37000$ (8.2 μm)	$\lambda/11600$ (2.6 μm)	$\lambda/3700$ (0.8 μm)	$\lambda/1265$ (237 nm)	$\lambda/320$ (94 nm)
Au	$\lambda/95000$ (32 μm)	$\lambda/30000$ (10 μm)	$\lambda/9500$ (3.2 μm)	$\lambda/3020$ (1.0 μm)	$\lambda/1010$ (297 nm)	$\lambda/300$ (100 nm)
Al	$\lambda/90000$ (33 μm)	$\lambda/28000$ (11 μm)	$\lambda/9000$ (3.3 μm)	$\lambda/2850$ (1.1 μm)	$\lambda/923$ (325 nm)	$\lambda/324$ (93 nm)
Cu	$\lambda/75000$ (41 μm)	$\lambda/23000$ (13 μm)	$\lambda/7500$ (4.1 μm)	$\lambda/2340$ (1.3 μm)	$\lambda/776$ (387 nm)	$\lambda/248$ (121 nm)

[a]The metals were characterized using the experimental data tabulated in [10].

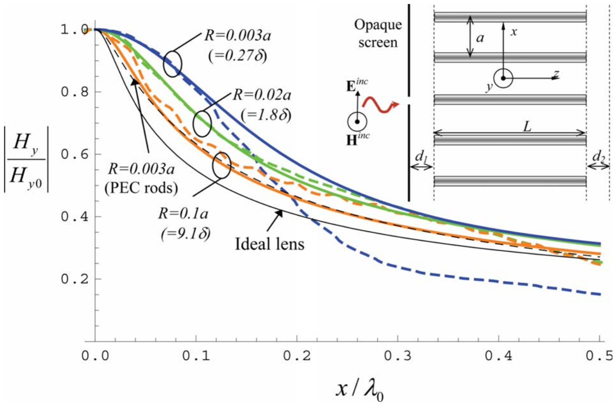

Fig. 1. (Color online) Normalized H_y at the image plane for different values of the rods' radius R. The geometry of the system is represented in the inset; the field transmitted through a subwavelength slit (at $x=0$) in an opaque screen is imaged by a wire medium slab at 5 THz. The metal is silver, and the lattice constant is $a=0.04\lambda_0=2.4$ μm. The black solid curves represent the results calculated with Eq. (5), whereas the black dashed curves represent the results obtained with CST Microwave Studio.

system may be greatly deteriorated when R becomes smaller than the skin depth. This confirms that when $R<\delta$ the resolution is not controlled by a, but instead by δ/R. The image created by very thin PEC rods with $R=0.003\lambda_0$ is also plotted in Fig. 1 (dashed black curve), which is similar to the image created by lossy rods with $R=0.1\lambda_0$ (orange curves) because R does not influence the resolution when the conductivity is sufficiently large.

In the second example (Fig. 2), the performance of the wire medium lens is illustrated when the image is a complex field distribution created by a source antenna shaped as the letters THz to emphasize the frequency of operation: 5 THz. Here, the lens is formed by an array of silver nanorods supported by a block of chalcogenide glass, which has low losses at terahertz frequencies. The calculated near-field distributions at the front and back interfaces are depicted in Figs. 2(b) and 2(c), respectively. The letters THz are clearly visible in both distributions. In fact, the radius of the rods was chosen so that $R/\delta=4.8$, which enables very good imaging. The resolution in this example is $\lambda/23$ (2.6 μm), and the image is formed at a distance 0.65λ (38.8 μm) from the source.

In conclusion, it is theoretically demonstrated that the resolution of imaging systems formed by metallic nanorods is ultimately determined by the skin depth of the metal and cannot be improved by reducing the lattice constant after the radius of the rods becomes smaller than the skin depth. It is anticipated that such near-field lenses may find applications in near-field microscopy and in medical imaging.

This work is supported in part by Fundação para a Ciência e a Tecnologia grant PDTC/EEA-TEL/71819/2006. P. Belov acknowledges financial support by the Engineering and Physical Sciences Research Council (UK) (EPSRC) Advanced Research Fellowship EP/E053025/1.

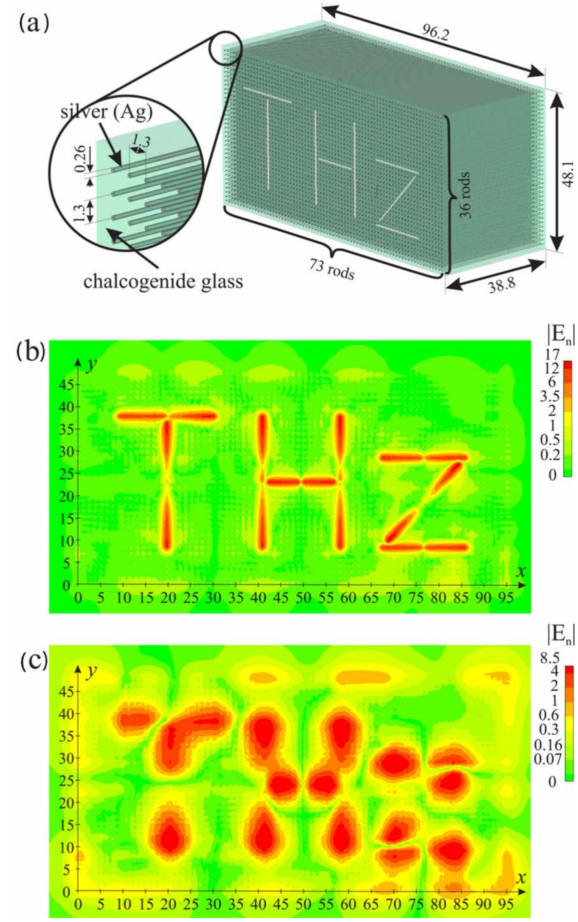

Fig. 2. (Color online) Numerical modeling of subwavelength imaging at 5 THz ($\lambda=60$ μm). (a) Geometry of the lens: a square array with a 1.3 μm period formed by silver nanorods with 130 nm radius embedded into a block of chalcogenide glass ($\varepsilon=2.2$). All dimensions in the figure are given in micrometers. The lens is excited by a planar antenna shaped in the form of the letters THz, and located 650 nm apart from the front interface of the lens. Calculated distributions of the normal component of electric field (b) at the front interface (source plane) and (c) at the back interface (image plane).

References

1. N. Fang, H. Lee, C. Sun, and X. Zhang, Science **308**, 534 (2005).
2. I. I. Smolyaninov, Y.-J. Hung, and C. C. Davis, Science **315**, 1699 (2007).
3. Z. Liu, H. Lee, Y. Xiong, C. Sun, and X. Zhang, Science **315**, 1686 (2007).
4. V. Westphal and S. W. Hell, Phys. Rev. Lett. **94**, 143903 (2005).
5. P. A. Belov, Y. Hao, and S. Sudhakaran, Phys. Rev. B **73**, 033108 (2006).
6. M. Silveirinha, P. Belov, and C. Simovski, Phys. Rev. B **75**, 035108 (2007).
7. P. A. Belov and M. G. Silveirinha, Phys. Rev. E **73**, 056607 (2006).
8. P. Belov, R. Marques, S. Maslovski, I. Nefedov, M. Silveirinha, C. Simovski, and S. Tretyakov, Phys. Rev. B **67**, 113103 (2003).
9. P. A. Belov, C. R. Simovski, and P. Ikonen, Phys. Rev. B **71**, 193105 (2005).
10. M. A. Ordal, R. J. Bell, R. W. Alexander, L. L. Long, and M. R. Querry, Appl. Opt. **24**, 4493 (1985).